Parameter sensitivity analysis of SWAT model for streamflow simulation with multisource precipitation datasets

Jing Guo and Xiaoling Su

ABSTRACT

Streamflow in the Shiyang River basin is numerically investigated based on the soil and water assessment tool (SWAT). The interpolation precipitation datasets of GSI, multisource satellite and reanalysis precipitation datasets including TRMM, CMDF, CFSR, CHIRPS and PGF are specially applied as the inputs for SWAT model, and the sensitivities of model parameters, as well as streamflow prediction uncertainties, are discussed via the sequential uncertainty fitting procedure (SUFI-2). Results indicate that streamflow simulation can be effectively improved by downscaling the precipitation datasets. The sensitivities of model parameters vary significantly with respect to different precipitation datasets and sub-basins. CN2 (initial SCS runoff curve number for moisture condition II) and SMTMP (base temperature of snow melt) are found to be the most sensitive parameters, which implies that the generations of surface runoff and snowmelt are extremely crucial for streamflow in this basin. Moreover, the uncertainty analysis of streamflow prediction indicates that the performance of simulation can be further improved by parameter optimization. It also demonstrates that the precipitation data from satellite and reanalysis datasets can be applied to streamflow simulation as effective inputs, and the dependences of parameter sensitivities on basin and precipitation dataset are responsible for the variation of simulation performance.

Key words | multisource datasets, sensitivity analysis, Shiyang River basin, streamflow simulation

Jing Guo
Xiaoling Su (corresponding author)
College of Water Resources and Architectural Engineering,
Northwest A&F University,
Yangling 712100,
China
E-mail: *xiaolingsu@nwsuaf.edu.cn*

Xiaoling Su
Key Laboratory for Agricultural Soil and Water Engineering in Arid Area of Ministry of Education,
Northwest A&F University,
Yangling 712100,
China

INTRODUCTION

Precipitation is well accepted as one of the most important input datasets for streamflow simulation using hydrological models (Liang *et al.* 2018). Generally, precipitation data can be obtained by ground stations, ground-based radars and remote sensing information. The precipitation data obtained by ground rainfall stations is accurate, but it is of heterogeneous spatial and temporal distributions due to the strong dependence on topography, wind direction, hill aspect and other regional factors (Price *et al.* 2014). Meanwhile, the precipitation data used in the soil and water assessment tool (SWAT) is typically adopted from the precipitation stations that are nearest to the centroid of the sub-basin without considering spatial heterogeneity (Neitsch *et al.* 2011), thus the spatial resolution of precipitation data is important for hydrological modelling. However, the sparse and heterogeneous spatial distribution of precipitation is difficult to evaluate accurately (Moine *et al.* 2015).

To improve the precision of precipitation data, spatial interpolation methods such as simple algorithmic averaging, Thiessen polygons, inverse distance weighting (IDW) and kriging interpolation, are proposed, and many models are established based on the spatial interpolation of

doi: 10.2166/nh.2019.083

meteorological observations with respect to the nonlinear relationships between precipitation and topographical factors, e.g. elevation, longitude and latitude (Teegavarapu & Chandramouli 2005). In recent years, due to the advantages of large spatial coverage, high spatial and temporal resolutions, and weak dependence on topographical conditions, meteorological data obtained from different sources, such as satellite and reanalysis, is extensively applied in the investigations on climate change, providing a new and feasible method to make up the disadvantages of observation data (Michaelides *et al.* 2009). The satellite and reanalysis precipitation datasets, e.g. Tropical Rainfall Measuring Mission (TRMM), Climate Forecast System Reanalysis (CFSR), Climate Hazards Group Infrared Precipitation with Stations (CHIRPS) and Global Meteorological Forcing dataset for land surface modelling developed by Princeton University (PGF) have been extensively applied when spatially heterogeneous precipitation data is used as the input data for hydrological models such as SWAT (Hu *et al.* 2014; Duan *et al.* 2016). The multisource precipitation data obtained by satellite and reanalysis, as an important supplement for precipitation datasets in hydrological models, can improve the simulation results. For instance, it indicates that the output error induced by the error of radar precipitation data is less than the error generated during the transition from precipitation to streamflow (Wyss *et al.* 1990). Nevertheless, except for the serious system errors possessed by the precipitation data, the accuracy of the retrieved precipitation is relatively low due to the limitations of the physical theories and algorithms for obtaining the satellite retrieved precipitation (Wang *et al.* 2018), and the uncertainty of precipitation input data will lead to the transfer and accumulation of uncertainty within different modules in hydrological models. For hydrological simulation at small scales, downscaling and deviation correction processing are usually applied to homogenize the spatial resolution of precipitation inputs (Wang *et al.* 2015).

Moreover, parameter optimization is the most important procedure during hydrological simulation because a large number of parameters are involved as the establishment of the hydrological model (Beck 1987), and every parameter is extremely crucial for the simulation results. Generally, model parameters are the comprehensive descriptions of the historical hydrological process and underlying surface properties (Beven & Binley 1992), and these parameters are obtained directly or indirectly from the basin properties, hydrological data and parameter optimization. However, the spatial heterogeneity of parameters, the errors induced during the acquisition process of hydrological data, and the errors caused by the selections of optimization method or objective function will reduce the accuracy of hydrological simulation and introduce serious uncertainties to the parameter initial values (Beven 1993). Meanwhile, the values of model parameters are highly related with each other and the phenomenon called 'parameters equifinality' occurs as a few groups of parameters correspond to the same fitting functions, which will increase the uncertainty of parameter values further. Therefore, the sensitivity analysis of model parameters is necessary to understand the effect of each parameter on simulation results during hydrological simulation (Jiang *et al.* 2018). Parameters can be reasonably selected according to the parameter sensitivity obtained by sensitivity analysis, which will reduce the number of parameters required in the calibration process and improve the simulation efficiency. More importantly, the parameter uncertainty and the output uncertainty can be effectively decreased.

The Shiyang River basin is a typical arid area with sparse rainfall stations, so precipitation data with high quality is required to obtain satisfactory simulation results of streamflow based on the SWAT model in this basin. In this study, the geographical spatial interpolation data of observed precipitation (GSI) and multisource precipitation datasets obtained by remote sensing and reanalysis, including TRMM, China Meteorological Forcing dataset (CMDF), CFSR, CHIRPS and PGF are specially considered as the input data for SWAT. Meanwhile, the multisource precipitation datasets are downscaled based on the GSI dataset, and the downscaled datasets are then applied to streamflow simulation to discuss whether it can be provided as the feasible precipitation input data or not. The sensitivities and uncertainties of model parameters using the downscaled precipitation inputs are discussed with respect to their effects on the results of streamflow simulation, so the prediction uncertainty of streamflow is also encountered to obtain the influences of parameters on the simulation performance under multisource precipitation datasets.

DATA AND METHODOLOGY

Study area

As illustrated in Figure 1, the Shiyang River basin is a typical arid inland basin that is located in Gansu Province (China) and covers an area of 41,400 km^2. The study area consists of six sub-basins located upstream of the Shiyang River basin, including the Xida River basin, Dongda River basin, Xiying River basin, Jintai River basin, Zamu River basin and Huangyang River basin. The basic meteorological data consists of precipitation, temperature, wind speed, solar radiation, and relative humidity obtained from the meteorological station of Wushaoling. Daily precipitation data was collected from 32 rain gauge stations (Figure 1(a)) for the period of 1989–2008. Streamflow data from 1990 to 2008 was obtained from six hydrological stations, including the Xidahe reservoir station, Shagousi station, Jiutiaoling station, Nanying reservoir station, Zamusi station, and Huangyang reservoir station, as shown in Figure 1(a). The spatial distributions of the land use and soil types in 2000

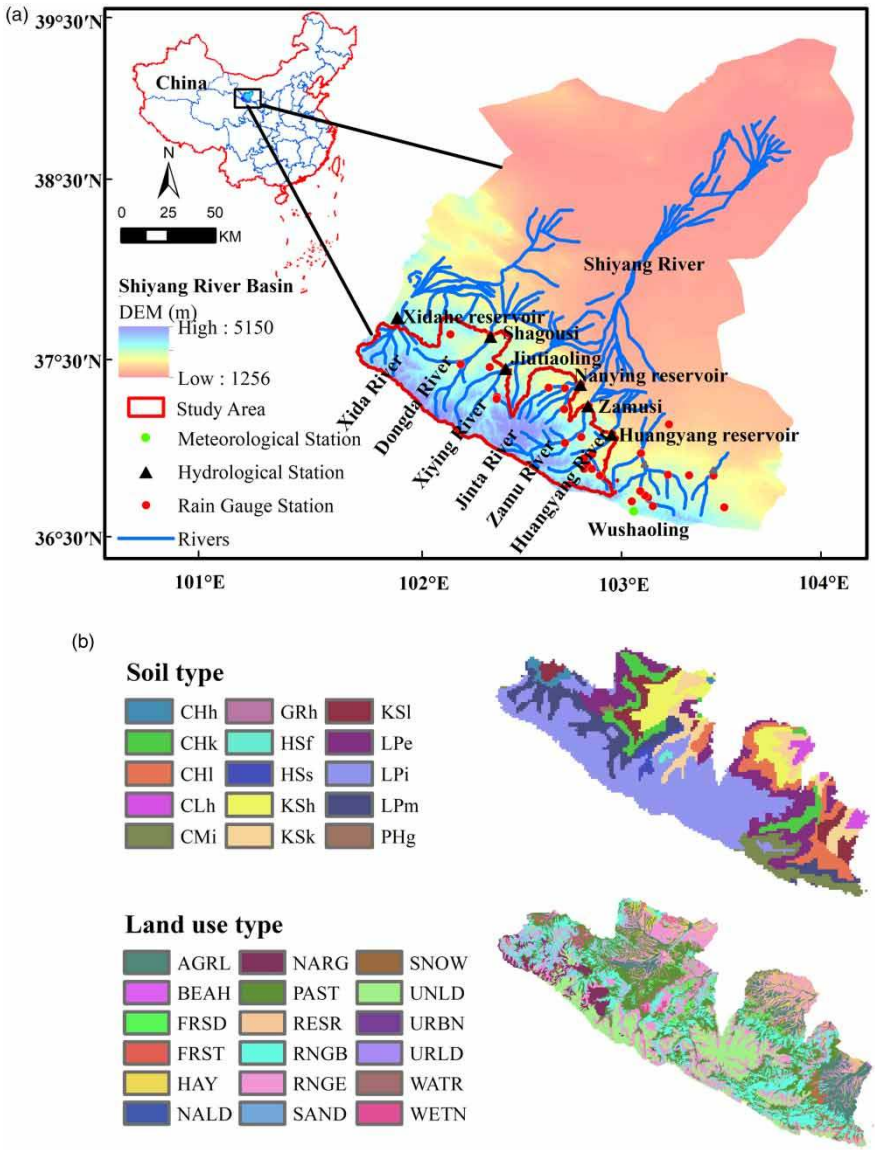

Figure 1 | Basic information of the Shiyang River basin: (a) basin overview and distribution of monitoring stations and (b) distributions of soil and land use types.

are shown in Figure 1(b), which indicates that there are 18 types of land use. The main land use categories are medium-coverage grasslands, high-coverage grasslands and shrubbery. Additionally, there are 15 soil types in this area, and the three main soil types are gelic leptosols, eutric leptosols and mollic gleysols. Details about the data required by the SWAT model can be found in Table 1.

Interpolation of observed precipitation

In this study, none of the rainfall stations is located at elevations higher than 3,000 m in the study area. For this reason, a geographical spatial interpolation method is established to estimate the spatial distribution of precipitation with respect to topographical factors derived from limited rainfall stations. The relationship between precipitation and elevation can be well captured by log-linear or exponential functions (Daly *et al.* 1994). In this study, the relationships among elevation, longitude, latitude and precipitation are taken into account in the interpolation method, and available precipitation data collected at 32 rainfall stations is used. The geographical spatial interpolation data of observed precipitation (GSI) can be obtained at a scale of 0.01°, and the annual precipitation data as a function of geomorphic factors is given by:

$$PCP = -132.5N_{lon} - 451.8N_{lat} + 30675.5\exp\left(\frac{3.69N_{ele}}{10^6}\right) \quad (1)$$

where PCP is the annual precipitation (mm), N_{lon} is the longitude of the rainfall stations, N_{lat} is the latitude, and N_{ele} denotes the elevation of the station (m).

Table 1 | Data sources and descriptions

Data type	Scale	Data source
Meteorological/ rainfall station data	Daily	Hydrology and Water Resources Bureau of Gansu Province
Streamflow	Monthly	Hydrology and Water Resources Bureau of Gansu Province
Digital elevation model (DEM)	90 × 90 m	United States Geological Survey (USGS)
Soil	1 × 1 km	Harmonized World Soil Database developed by the Food and Agriculture Organization (FAO) and International Institute for Applied Systems Analysis (IIASA)
Land use	30 × 30 m	Geographical Information Measured Cloud Platform (satellite remote sensing image data from Landsat TM)

Multisource datasets and downscaling

Satellite and reanalysis precipitation datasets including TRMM, CMDF, CFSR, CHIRPS and PGF were used in this study, and the detailed information of each dataset is summarized in Table 2. Specifically, TRMM 3B42, as one kind of TRMM multi-satellite precipitation analysis (TMPA) dataset (Huffman *et al.* 2007), can be obtained from the Goddard Earth Sciences Data and Information Services Center at http://mirador.gsfc.nasa.gov. The CMDF data, provided by the Data Assimilation and Modelling Center for Tibetan multi-spheres (DAM), is produced by merging data series, including the existing Princeton reanalysis data, Global Land Data Assimilation System (GLDAS) data, Global Energy and Water Cycle Experiment-Surface Radiation Budget (GEWEX-SRB) data, TRMM precipitation data and routine meteorological observations from the China Meteorological Administration (Li *et al.* 2012). The CFSR data, provided by the National Centers for Environmental Prediction, is designed and implemented as a global, high-resolution, coupled atmosphere–ocean–land surface–sea-ice system to provide the best estimations of the states of these coupled domains (Saha *et al.* 2010), available at https://rda.ucar.edu/pub/cfsr.html. The CHIRPS data is based on the integration of various datasets and is available at http://chg.geog.ucsb.edu/data/chirps/. Actually, the CHIRPS data includes the monthly precipitation climatology (CHPclim) data, the cold cloud duration (CCD) information, the TRMM 3B42 data (version 7), the atmospheric rainfall model (version 2) and the rain station data (Funk *et al.* 2015). The PGF dataset, available at http://hydrology.princeton.edu/data.pgf.php, can be constructed using four datasets, including the NCEP reanalysis data, Climatic Research Unit (CRU)

Table 2 | Precipitation obtained from satellite and reanalysis data

Dataset	Period	Spatial resolution	Temporal resolution	Coverage	Category
TRMM	1998–2010	0.25°	3 hour	50° N–50° S	Satellite station
CMDF	1979–2010	0.01°	3 hour	50° N–50° S	Reanalysis gauge
CFSR	1979–2009	0.30°	6 hour	90° N–90° S	Reanalysis gauge
CHIRPS	1981–2010	0.05°	Daily	50° N–50° S	Satellite station
PGF	1948–2010	0.25°	3 hour	90° N–90° S	Reanalysis gauge

monthly precipitation data, Global Precipitation Climatology Project (GPCP) daily precipitation data and TRMM 3-hour real-time data (Sheffield *et al.* 2006).

As shown in Table 2, these datasets are different in the spatial resolution that ranges from 0.01 to 0.3°, which may impact on the accuracy of streamflow simulation to different extents (Li *et al.* 2012). Hence, the downscaling or deviation correction processing is performed to improve the accuracy of precipitation data (Cecinati *et al.* 2017). For the downscaling process, the spatial interpolation data of precipitation (GSI) obtained via the method of geographical spatial interpolation is used as the base data. Then, the satellite and reanalysis precipitation datasets can be corrected at the spatial resolution of 0.01° by the offset adjustment factor as follows:

$$R_{ij,radar} = R_{ij,day} \cdot \frac{R_{i,radar}}{R_{i,gauge}} \tag{2}$$

where $R_{ij,radar}$ is the precipitation on the jth day in month i recorded at the radar data location (mm), $R_{ij,day}$ is the precipitation on the jth day in month i recorded at the gauge station (mm), $R_{i,radar}$ is the average precipitation in month i obtained from the radar datasets, and $R_{i,gauge}$ represents the average precipitation in month i obtained from the gauge data.

Method of SUFI-2

The parameters considered in the Bayesian statistical theory are taken as a group of fuzzy variables which are related to the joint posterior probability density (He *et al.* 2011). Thus, the parameter uncertainty can be quantified by the posterior probabilities of model parameters, the prior information contained by model parameters and the information contained by input data (Misirli *et al.* 2013). Among the method of sensitivity and uncertainty analyses of parameters, SUFI-2 (sequential uncertainty fitting procedure, version 2) is an efficient global search algorithm for calibration, parameter optimization and uncertainty analysis with a low computational cost (between 500 and 1,500 model runs) (Abbaspour 2011), and all of these can be achieved based on the SWAT-Calibration Uncertainty Programs (CUP) tool package. In SUFI-2, the parameter optimization is applied to a parameter set and the parameter uncertainties are described by the final ranges of the parameter sets (Abbaspour 2011), and generally, the optimization algorithms include the simplex method, random searching algorithm and competitive coevolutionary algorithm (Duan *et al.* 1992), and the global analysis methods of LH (Latin-Hypercube) is used in SUFI-2 (Abbaspour 2011).

The procedure of SUFI-2 includes: (1) define the objective function and initial ranges of the parameters, where initial values are empirical; (2) provide new parameter values for the subsequent operation by the correlation between the objective function and the parameters, where multiple simulations of each parameter are performed; (3) obtain the multiple combinations of parameters based on LH sampling, and the 95% prediction interval of each parameter is determined; (4) calculate the 95% prediction uncertainty (95PPU). During these processes, the sensitivity matrix is determined by:

$$j_{ij} = \frac{\Delta g_i}{\Delta b_j},\ i = 1 \ldots, C_2^n,\ j = 1,\ \ldots, m \tag{3}$$

where i is the group number of LH, j is the parameter number, C_2^n is the number of rows in the sensitivity matrix, Δb_j is the jth parameter that needs to be calibrated, Δg_i is the sensitivity of parameter.

The Hessian matrix is calculated by:

$$H = J^T J \tag{4}$$

The covariance matrix C is determined by:

$$C = s_g^2 (J^I J) \tag{5}$$

where s_g^2 is the variance of objective function after n simulations. Thus, the standard deviation and 95% confidence interval of parameter b_j can be further determined by:

$$s_j = \sqrt{C_{jj}} \tag{6}$$

$$b_{j,lower} = b_j^* - t_{v,0.025} \cdot S_j \tag{7}$$

$$b_{j,upper} = b_j^* - t_{v,0.025} \cdot S_j \tag{8}$$

where b_j^* is the optimal solution of parameter b, and v is the degree of freedom ($n-m$).

The sensitivity and significance of each parameter are evaluated by the t-value and P-value, respectively. The t-value describes the behaviour of a sample that is composed of a certain number of observations. The P-value tests the null hypothesis. If the P-value is <0.05, the null hypothesis is rejected, while the parameter impacts on the results with a 95% probability if the P-value equals 0.05. Moreover, a parameter with a large t-value and small P-value is suggested to be sensitive to streamflow (Abbaspour 2011).

In this study, 25 parameters from five process categories, including groundwater, runoff, evaporation, channel and snow, are selected for the sensitivity and uncertainty analyses in SWAT, as listed in Table 3, where the prefix 'v_' indicates that the parameter value is replaced by a given value or an absolute change, and 'r_' indicates that the parameter value is either multiplied by 1 + a given values or denotes a relative change. The initial parameter ranges are set according to the SWAT manual, as well as previous investigations in the literature (Arnold *et al.* 2012).

Uncertainty of streamflow simulation

Generally, the uncertainties of the streamflow prediction introduced by driving variables (e.g. rainfall), model structure and model parameters data can be taken into account by the SUFI-2 algorithm. The prediction uncertainties are quantified by the prediction uncertainty bands, and it is evaluated by two factors, i.e. the P-factor and R-factor, among which the P-factor denotes the percentage of measured data covered by the 95% confidence interval (95% prediction uncertainty, 95PPU). The band width of 95PPU is given by:

$$\overline{d_x} = \frac{1}{k} \sum_{i=1}^{k} (x_u - x_l)_i \tag{9}$$

where x is the simulation value of streamflow, k is the number of streamflow simulation, x_l is the lower limit of 95PPU that corresponds to the 2.5% probability at the cumulative probability curve, and x_u is the upper limit of 95PPU that corresponds to the 97.5% probability at the cumulative probability curve. It can be easily found that P-factor approaches to 1 if the observation data all locates within the 95PPU and thus $\overline{d_x}$ approaches to 0. The R-factor, representing the thickness of the 95PPU envelope or the ratio of the average width of the 95PPU band to the standard deviation of the measured variable, is determined by:

$$R - factor = \frac{\overline{d_x}}{\sigma_x} \tag{10}$$

where σ_x is the standard deviation of streamflow observation data x. The value of R-factor shows the distribution property of simulated streamflow, i.e. the simulated streamflow distributes loosely with respect to the streamflow observations as the R-factor is large, in contrast, it distributes closely as the R-factor is small. In particular, the simulation results are totally consistent with observation data as P-factor equals 1 and R-factor equals 0, and for streamflow simulation, P-factor >0.7 and R-factor <1.5 are considered to be acceptable for prediction uncertainty (Abbaspour 2011).

SWAT model setup

SWAT is a hydrological model that has been proven to be able to obtain the detailed hydrological information in a

Table 3 | Parameters used in the sensitivity analysis

Parameter	Meaning of parameter	Initial range	Classification
v_SMFMN	Minimum melt rate for snow during the year (occurs on winter solstice)	0–20	Snow melt
v_SMFMX	Maximum melt rate for snow during the year (occurs on summer solstice)	0–20	Snow melt
v_SMTMP	Base temperature of snow melt	–20–20	Snow melt
v_TIMP	Snow pack temperature lag factor	0–1	Snowfall
v_SFTMP	Snowfall temperature	–20–20	Snowfall
r_CN2	SCS runoff curve number for moisture condition II	–0.1–0.1	Surface runoff
v_SURLAG	Surface runoff lag time	0.05–24	Surface runoff
v_ALPHA_BF	Baseflow alpha factor (days)	0–1	Groundwater
v_REVAPMN	Threshold depth of water in the shallow aquifer for 'revap' to occur (mm)	0–500	Groundwater
v_GW_DELAY	Groundwater delay (days)	0–500	Groundwater
v_GW_REVAP	Groundwater 'revap' coefficient	0.02–0.2	Groundwater
v_RCHRG_DP	Deep aquifer percolation fraction	0–1	Groundwater
v_GWQMN	Threshold depth of water in the shallow aquifer required for return flow to occur (mm)	0–1,000	Groundwater
v_EPCO	Plant uptake compensation factor	0–1	Evapotranspiration
v_ESCO	Soil evaporation compensation factor	0–1	Evapotranspiration
v_SLOPE	Average slope	0–90	Landform
v_SLSUBBSN	Average slope length	10–150	Landform
v_TLAPS	Temperature lapse rate	–10–10	Temperature
v_ALPHA_BNK	Baseflow alpha factor for bank storage	0–1	Channel
v_CH_K2	Effective hydraulic conductivity in main channel alluvium	0.01–500	Channel
v_CH_N2	Manning's 'n' value for the main channel	0.01–0.3	Channel
v_SOL_AWC	Available water capacity of the soil layer	0–1	Soil
v_SOL_K	Saturated hydraulic conductivity	0–500	Soil
v_CANMX	Maximum canopy storage	0–50	Vegetation
v_BLAI	Max leaf area index	0.5–10	Vegetation

basin (Silva *et al.* 2018). In this study, streamflow is simulated by SWAT with an ESRI QGIS interface (Dile *et al.* 2016). The modified Soil Conservation Service (SCS) curve number method is used to calculate the surface streamflow. Snowmelt is estimated by the energy balance equation. Potential evapotranspiration is determined by the Hargreaves method, and channel routing is simulated by a variable storage method (Neitsch *et al.* 2011). For monthly streamflow simulations using SWAT, three years from 1987 to 1989 are used as the warm-up period to mitigate the effects of unknown initial conditions, and the periods of 1990–2000 and 2001–2008 are selected as the calibration period and validation period, respectively.

The precipitation data used in the SWAT model includes three categories: (a) geographical spatial interpolation data of observed precipitation (GSI); (b) the original satellite and reanalysis precipitation datasets; and (c) the downscaled satellite and reanalysis precipitation datasets. The models that use different precipitation datasets as input data for SWAT modelling are labelled as M_{GSI}, M_{TRMM}, M_{CMDF}, M_{CFSR}, M_{CHIRPS} and M_{PGF}, where the subscript denotes the dataset name.

The Nash–Sutcliffe coefficient (*NS*), is applied to evaluate the performance of model simulation. According to the value of the *NS* coefficient, the model performance can be divided into different categories, including unsatisfactory performance ($NS \leq 0.50$), satisfactory performance ($0.50 < NS \leq 0.65$), good performance ($0.65 < NS \leq 0.75$) and very good performance ($0.75 < NS \leq 1.00$) (Moriasi *et al.* 2007). In addition to the *NS*, the coefficient of determination (R^2)

is also used to assess the fitting of the observation values and simulation results.

RESULTS AND DISCUSSION

Streamflow simulation and evaluation

Streamflow simulations of six sub-basins in the Shiyang River basin based on SWAT model are performed using the GSI, original and downscaled satellite and reanalysis precipitation datasets. Figure 2 shows the monthly streamflow simulations in the calibration period with respect to the Xida River basin, Dongda River basin, Xiying River basin, Jinta River basin, Zamu River basin, and Huangyang River basin. Herein, the simulation results obtained by different precipitation datasets are compared with observation data. As can be seen from Figure 2(a), 2(c), 2(e), 2(g), 2(i) and 2(k), all five precipitation dataset models fail to reproduce the discharge records before downscaling, and based on the *NS* values shown in Figure 3, it also indicates that all the dataset models present unsatisfactory performance before downscaling. This can be interpreted by the fact that the spatial variability in precipitation patterns can be poorly captured because the topographic effects are not taken into consideration before downscaling.

However, as shown in Figure 2(b), 2(d), 2(f), 2(h), 2(j) and 2(l), the performances of these models can be significantly improved after downscaling, which can also be observed from the *NS* values of these models shown in Figure 3. It indicates that downscaling based on the GSI dataset tends to yield larger *NS* and R^2 values for different models in all sub-basins, and it is also found that most values of R^2 increase slightly after downscaling, while the *NS* values increase significantly for most models in most sub-basins.

Moreover, Figure 3 also indicates that M_{GSI} performs best among all the models in the Xida, Dongda and Jinta River basins, and M_{CMDF} performs best in the Xiying, Zamu and Huangyang River basins. The most obvious increases in *NS* and R^2 values after downscaling are obtained by M_{CMDF} and M_{PGF}, while the *NS* and R^2 values change a little for M_{CFSR} and M_{CHIRPS} before and after downscaling. Additionally, the *NS* and R^2 values are also found to decrease after downscaling such as when using M_{CFSR} and M_{CHIRPS} in some sub-basins, and this indicates that the heterogeneous patterns and intensities of precipitation are not completely eliminated from the original datasets. Therefore, the spatial accuracy of the precipitation observation data and the quality of most precipitation data from the satellite and reanalysis datasets are improved by the geographical spatial interpolation, except for the data from the CFSR and CHIRPS datasets in some sub-basins. Hence, it is also found that the geographical spatial interpolation is feasible for estimating the precipitation in areas lacking observed data in Shiyang River basin. In general, the five satellite and reanalysis precipitation datasets after downscaling are feasible for streamflow simulation in the Shiyang River basin.

Sensitivities of model parameters

Sensitivity analysis is carried out for model parameters to determine the influence of each parameter on the performance of streamflow simulation. The three most sensitive parameters and their values during the runoff simulation in the Xida River using multisource precipitation inputs, i.e. GSI, TRMM, CMDF, CFSR, CHIRPS and PGF, are listed in Table 4. It can be found that the most sensitive parameter in the Xida River is SMTMP, which indicates that the runoff simulation is very sensitive to the snow melting temperature. The value as well as varying range of this parameter change with different precipitation inputs, lying between −0.94 and 9.84. Moreover, ALPHA_BNK ranks second, third and third for GSI, CMDF and CHIRPS, respectively. GW_REVAP, GWQMN, RCHRG_DP, SMFMX and TIMP are found to be the most sensitive parameters for multisource precipitation inputs, among which the former three are groundwater parameters, and the latter two are snowmelt runoff parameters. Therefore, the most sensitive parameters in the Xida River are ice and snow melting, groundwater recharge and river base flow, and snowmelt runoff and groundwater recharge are very important for runoff production in the Xida River.

Similarly, the three most sensitive parameters in the Dongda River, Xida River, Xiying River, Jinta River, Zamu River and Huangyang River under the precipitation datasets of GSI, TRMM, CMDF, CFSR, CHIRPS and PGF are

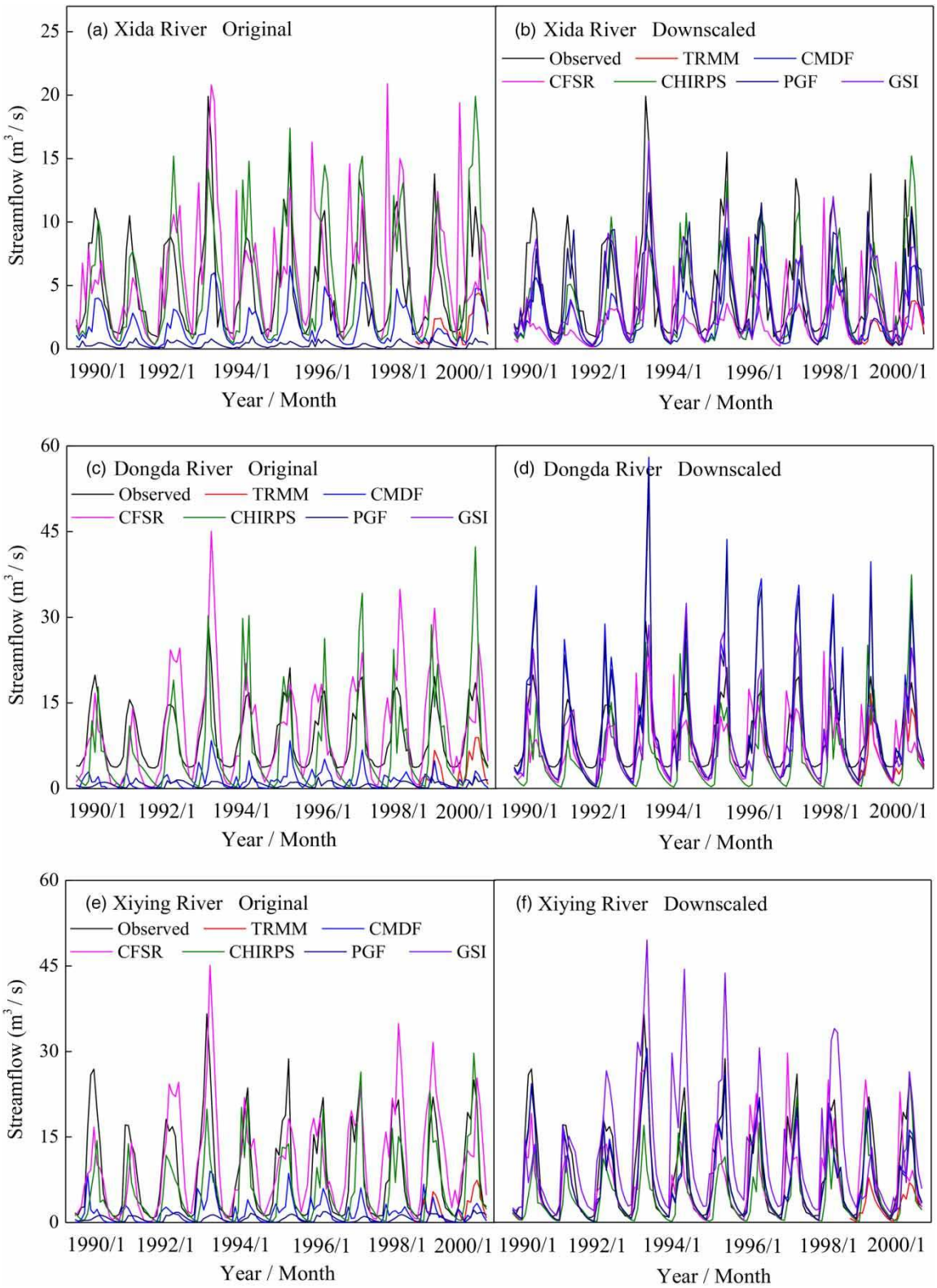

Figure 2 | Comparison of observation data and streamflow simulation using original and downscaled precipitation datasets in the six sub-basins. (*Continued*.)

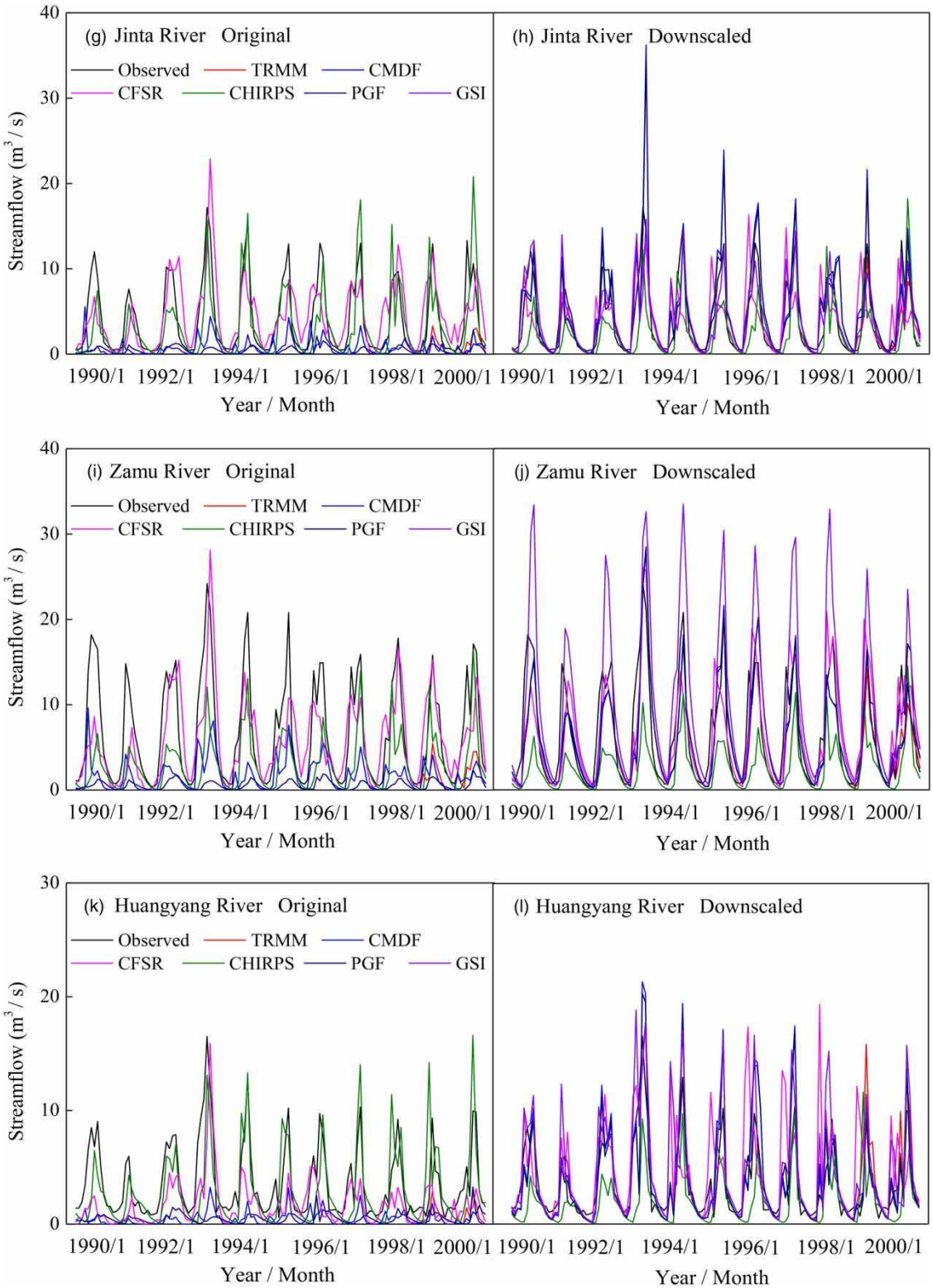

Figure 2 | Continued.

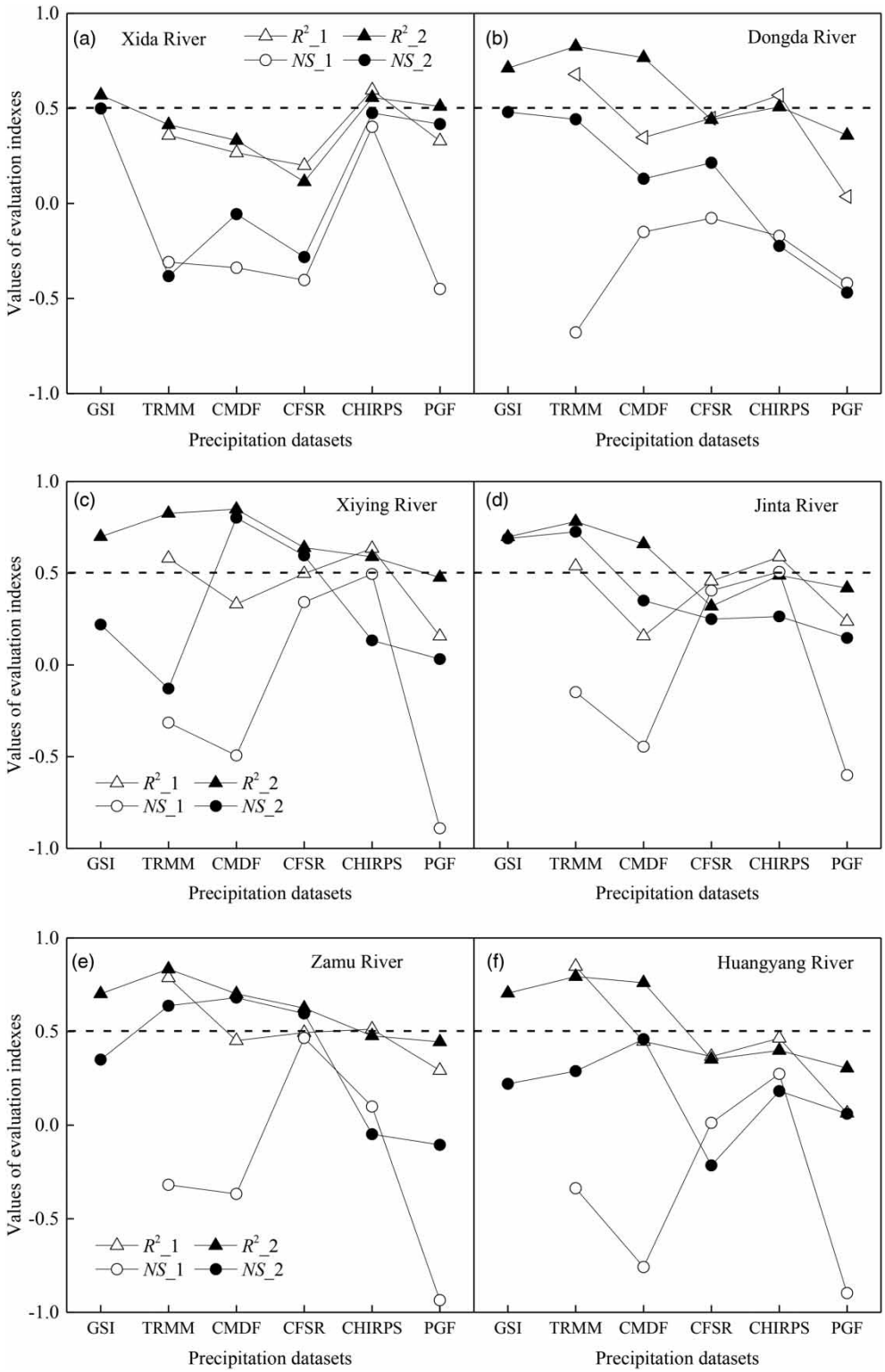

Figure 3 | The values of R^2 and *NS* for streamflow simulations based on different datasets before (open symbols) and after (solid symbols) downscaling in six sub-basins.

Table 4 | Sensitivity analysis of model parameters and its final value range under multi-source precipitation datasets in Xida River basin

Datasets	Rank	Parameter	*t*-stat	*p*-stat	Fitted_value	new_min	new_max
GSI	1	SMTMP	13.30	<0.01	4.85	–0.08	9.78
	2	ALPHA_BNK	8.07	<0.01	0.24	–0.14	0.62
	3	GW_REVAP	–4.99	<0.01	0.14	0.08	0.20
TRMM	1	SMTMP	16.76	<0.01	4.11	–0.45	8.66
	2	GW_REVAP	–16.00	<0.01	0.12	0.07	0.16
	3	GWQMN	–15.38	<0.01	149.1	–76.37	374.57
CMDF	1	SMTMP	18.14	<0.01	4.69	–0.16	9.54
	2	RCHRG_DP	–16.11	<0.01	0.28	–0.09	0.64
	3	ALPHA_BNK	13.82	<0.01	0.82	0.41	1.23
CFSR	1	SMTMP	20.03	<0.01	4.68	–0.16	9.51
	2	SMFMX	–16.72	<0.01	0.01	–4.99	5.01
	3	TIMP	–6.68	<0.01	0.48	0.23	0.74
CHIRPS	1	SMTMP	19.49	<0.01	4.89	–0.06	9.84
	2	RCHRG_DP	14.09	<0.01	0.86	0.43	1.28
	3	ALPHA_BNK	10.71	<0.01	0.63	0.31	0.94
PGF	1	SMTMP	14.30	<0.01	3.13	–0.94	7.19
	2	GWQMN	–9.85	<0.01	323.50	161.70	485.30
	3	GW_REVAP	–8.82	<0.01	0.04	–0.04	0.12

obtained, as shown in Figure 4. For the Dongda River, the most sensitive parameters are SMTMP, CN2, CN2, SMFMX, CN2, CN2 for the precipitation datasets GSI, TRMM, CMDF, CFSR, CHIRPS and PGF, respectively. Moreover, RCHRG_DP, ESCO and ALPHA_BNK belong to the top three sensitive parameters using multisource precipitation inputs. This indicates that the most sensitive parameters in the Dongda River are surface runoff, snowmelt, groundwater recharge and evaporation. For the Xiying River, the most sensitive parameters are RCHRG_DP, CN2, SMTMP, SMTMP, CH_K2 and CN2 for the six precipitation datasets, respectively. Moreover, the top three sensitive parameters include GW_DELAY, ALPHA_BNK, SMFMX, TIMP, ESCO and ALPHA_BF, which indicates that the most sensitive parameters in the Xiying River are surface runoff, snowmelt, groundwater recharge, river base flow and evaporation. For the Jinta River, the most sensitive parameters respectively are SMFMX, CN2, SMTMP, SMFMX, CN2 and CN2 for the six precipitation datasets. The top three sensitive parameters also include TIMP, CH_K2 and ESCO, and thus snowmelt, surface runoff, river base flow and evaporation are the most sensitive parameters in the Jinta River. For the Zamu River, the most sensitive parameters are SMTMP, CN2, SMTMP, SMFMX, CN2 and CN2 for the six

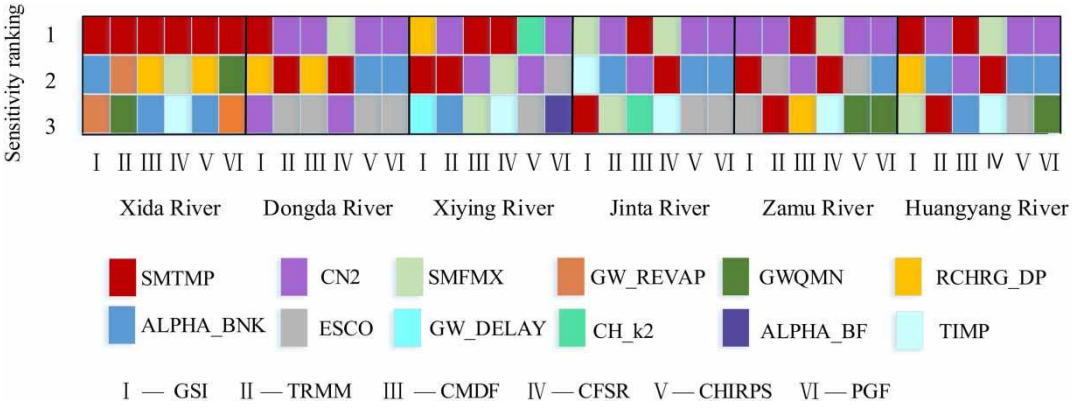

Figure 4 | Sensitivity analysis of the parameters using six different datasets (x-axis) in six sub-basins, where 1, 2, and 3 in y-axis represent the ranking of sensitivity.

precipitation datasets, respectively. The top three sensitive parameters also include RCHRG_DP, ALPHA_BNK, TIMP and ESCO, and this indicates that surface runoff, snowmelt, groundwater recharge, river base flow and evaporation are the most important parameters in the Zamu River. For the Huangyang River, the most sensitive parameters are CN2, CN2, SMTMP, SMFMX, CN2 and CN2 for the six precipitation datasets, and RCHRG_DP, ALPHA_BNK, GWQMN also belongs to the top three sensitive parameters, which indicates the most sensitive parameters in the Huangyang River are surface runoff, snowmelt, evaporation, groundwater recharge and river base flow.

As can be found in Figure 4, the sensitivities of most parameters vary significantly with respect to different sub-basins and precipitation datasets. Thus it is impossible to obtain a general answer of parameter sensitivity ranking for all precipitation datasets, even in the same sub-basin. However, among all the sensitivity parameters, due to the similarities in hydrological behaviour associated with similar geographic and climatic environments of different sub-basins, CN2 and SMTMP show the highest relative sensitivity for most of the sub-basins when using multisource precipitation datasets, which suggests that the surface runoff and snowmelt are of significant importance for the streamflow production in the Xida River, Dongda River, Xiying River, Jinta River, Zamu River and Huangyang River.

Uncertainty analysis of parameters

Furthermore, the uncertainty analysis of parameters obtained by the SUFI-2 procedure is also performed. The selected values of different parameters for different datasets and sub-basins are shown in Figure 5, where the ranges of parameter value are also provided. Parameters here include CN2, SMTMP, ALPHA_BNK, ESCO, SMFMX and RCHRG_DP. It is obvious that, even in the same sub-basin, the selected value and value range of most parameters vary significantly with respect to different dataset models. For instance, the CN2 has larger selected values in the cases of M_{TRMM}, M_{PGF} and M_{CHIRPS}, while in M_{CMDF} it is of the lowest value. The selected values of SMTMP for different datasets in the Xida River and Dongda River basins change over a small range when compared with those in other sub-basins. Moreover, the values of ALPHA_BNK are considered to be reasonable in all sub-basins. The high value of ESCO indicates that there is a high evaporation compensation in the soil, and this is consistent with the climatic, geographical and environmental conditions in the mountainous areas of sub-basins. In addition, SMFMX and RCHRG_DP show changes for different datasets and sub-basins.

However, the evaluation of the selected parameter value is associated with inherent uncertainty. Due to the model assumptions, it is typically impractical to define parameter values based on estimations according to probability distributions. Moreover, in this study, the parameter values are significantly different for the same basin when the model is calibrated using different precipitation datasets. Despite the similarities in land use, major soil types and other hydrological and meteorological conditions in all the sub-basins, the parameter values are also different for the same precipitation dataset in different sub-basins. Thus, it is impossible to apply the outcomes obtained in one sub-basin to all sub-basins. In other words, the parameter uncertainty is closely related to the properties of the basin. The results indicate that the selected value and its ranges of most parameters vary significantly with respect to different sub-basins and dataset models, which reflects the uncertainty of the model parameters and the variation of simulation performance under multisource precipitation datasets.

Evaluation of streamflow prediction and uncertainty

The performances of the precipitation datasets after downscaling for streamflow prediction with parameter optimization in the Xiying River basin are further investigated. Comparisons of the best streamflow simulations and observation data in the Xiying River basin considering different precipitation datasets are shown in Figure 6, where the black lines denote the measured streamflow and red ones denote the best streamflow simulations. Figure 6 also shows the uncertainties of streamflow prediction during the calibration period, where the green shaded area represents 95PPU. It should be noted that the TRMM dataset is limited by the time scale, thus only the data of TRMM in the period of 1999–2008 is used to simulate the streamflow.

The values of evaluation indexes of the streamflow simulation for different dataset models can also be found in Figure 6, which indicates that the six datasets have R^2 values

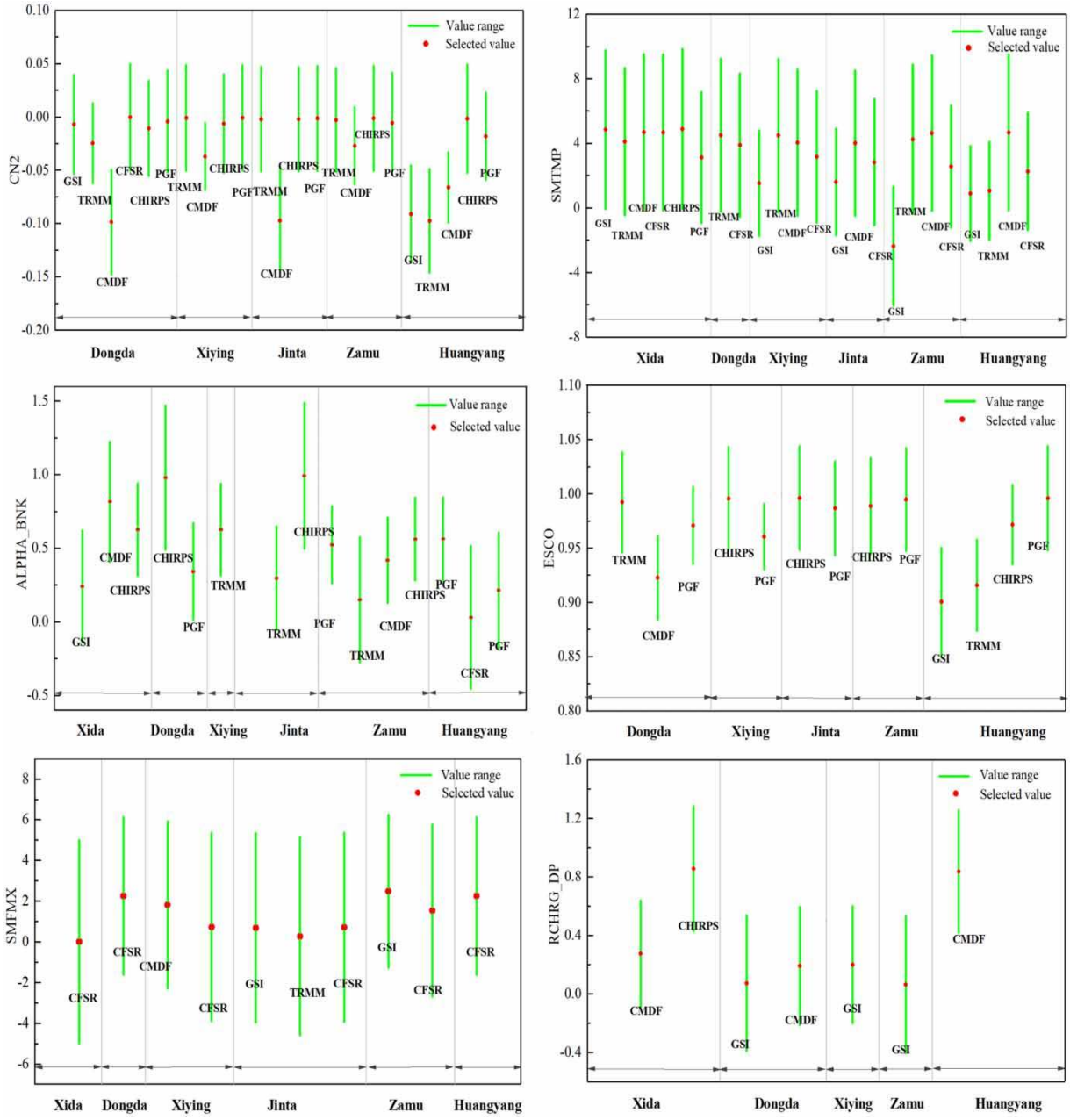

Figure 5 | Parameter values with respect to different datasets in different sub-basins, where the green bars denote the final parameter ranges and the red points are the best value of the parameter. Please refer to the online version of this paper to see this figure in colour: http://dx.doi.org/10.2166/nh.2019.083.

greater than 0.6 and *NS* values greater than 0.5 during the calibration and validation period in the Xiying River basin. Considering the value of *NS*, the simulation performances using different precipitation datasets in the calibration period are in the rank of $M_{CMDF} > M_{TRMM} > M_{CHIRPS} > M_{CFSR} > M_{PGF} > M_{GSI}$, and in the validation period, the sequence is $M_{CFSR} > M_{GSI} > M_{CMDF} > M_{CHIRPS} > M_{PGF}$. Particularly, the performance of the SWAT model is better during the validation period than the calibration period in the cases of M_{GSI}, and other dataset models show better performance during the calibration period. One possible reason for this is that the distribution of precipitation during the calibration and validation periods is different for the six datasets. Moreover, the *NS* and R^2 in the case of parameters optimization

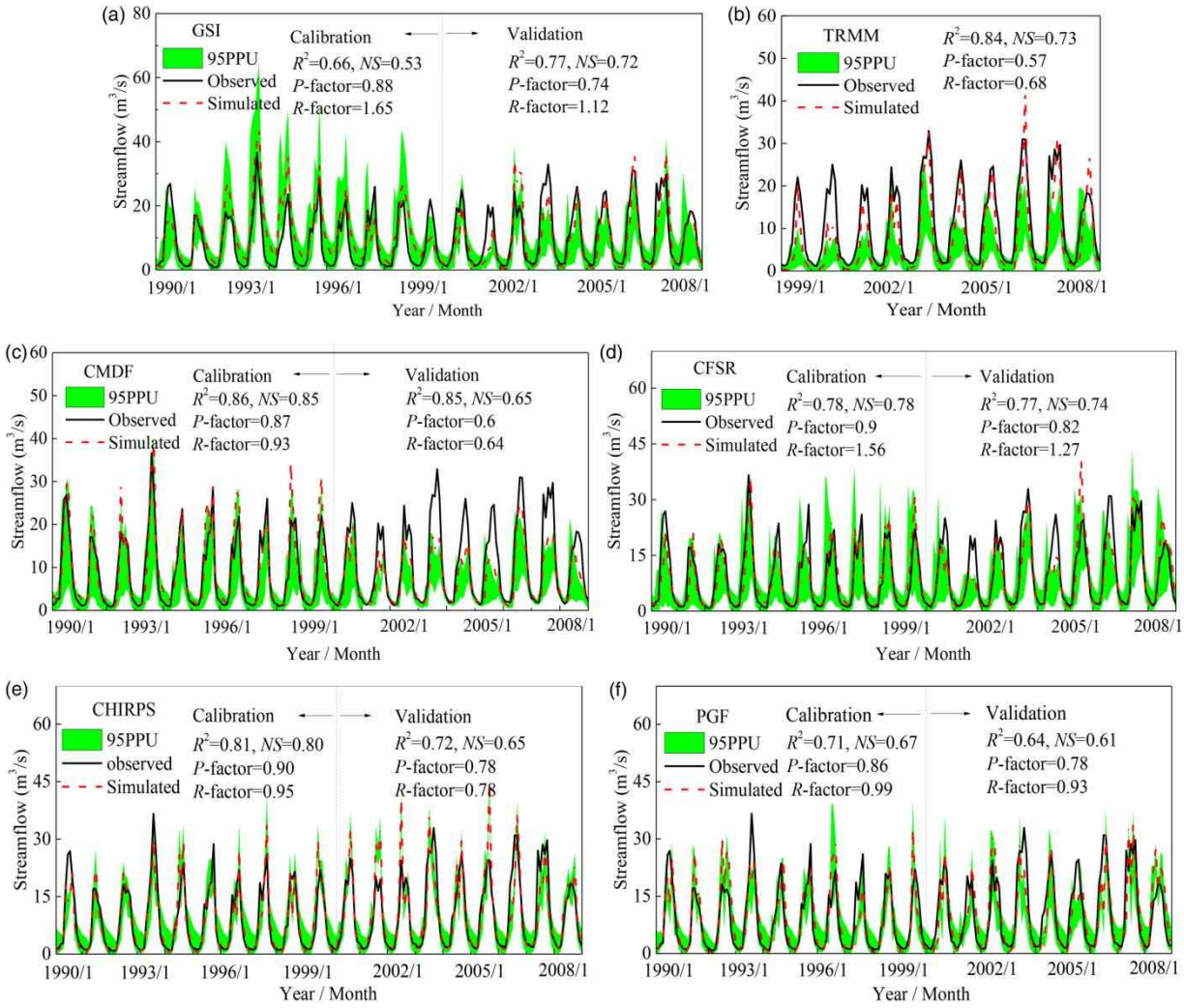

Figure 6 | SUFI-2 prediction uncertainty bounds for different precipitation datasets after downscaling during the calibration period in the Xiying River basin. Please refer to the online version of this paper to see this figure in colour: http://dx.doi.org/10.2166/nh.2019.083.

are greater than those before parameter adjustment in the calibration period.

For streamflow simulation using M_{GSI} in the Xiying River basin, the timing and magnitude of flows are reasonably captured. Moreover, the M_{CFSR} model shows the best performance, and the values of *NS* are 0.78 and 0.74 in the calibration and validation periods, respectively. The streamflow simulations in the Xiying River basin using different precipitation datasets indicate that most overestimates appear in summer (i.e. June, July and August), and underestimates are more likely occur in December and January for most dataset models. In general, all the models using the six datasets are able to reproduce the observation data of streamflow in the Xiying River basin, and most of them are of consistent and satisfactory performance. The simulation results can be improved by adjusting the relevant hydrological parameters to their optimal calibrated values based on SWAT-CUP. Furthermore, the accuracy of the precipitation input impacts on the accuracy of the simulation results, and satellite and reanalysis datasets are suggested to be reasonable inputs for hydrological simulation at basin scale, especially for the basins with a lack of rainfall gauges.

Uncertainties in streamflow prediction during the calibration and validation periods using different precipitation datasets in the Xiying River basin are also shown in Figure 6, where the 95PPU contains all uncertainties from different

sources. For the calibration period, the results indicate that the *P*-factor values of M_{GSI}, M_{TRMM}, M_{CMDF}, M_{CFSR}, M_{CHIRPS}, M_{PGF} are 0.88, 0.57, 0.87, 0.9, 0.9 and 0.86, respectively, and the *R*-factor values are 1.65, 0.68, 0.93, 1.56, 0.95 and 0.99, respectively. For the validation period, it also shows an acceptable performance with *P*-factor of M_{GSI}, M_{CMDF}, M_{CFSR}, M_{CHIRPS}, M_{PGF} being 0.74, 0.6, 0.82, 0.78 and 0.78, respectively, and *R*-factor of 1.12, 0.64, 1.27, 0.78 and 0.93, respectively. Thus most of the observation data can be covered by the 95PPU.

In the calibration period, it indicates that M_{TRMM} has the smallest *P*-factor (i.e. 0.57) among all datasets, which means that only 57% of simulated streamflow is covered by the 95% streamflow prediction uncertainty band. The values of *R*-factor with respect to most dataset models are less than 1, which means that the streamflow simulation distributes closely with respect to the streamflow observations as the *R*-factor is smaller than 1.5, except for the models using M_{GSI} and M_{CFSR} and it may be caused by the large uncertainty in simulating the streamflow peaks. Thus the prediction uncertainties using M_{CMDF}, M_{CHIRPS} and M_{PGF} are acceptable. While in the validation period, except for the model using CMDF where the *P*-factor is less than 0.7, the *P*-factor and *R*-factor values of other precipitation datasets are acceptable, indicating that the prediction uncertainties using M_{GSI}, M_{CFSR}, M_{CHIRPS} and M_{PGF} are acceptable.

Moreover, for both the calibration and validation periods, it is obvious that M_{CHIRPS} and M_{PGF} are able to achieve a good balance between the *P*-factor and *R*-factor, which shows acceptable and satisfactory uncertainties of streamflow predictions. However, in the validation period, some streamflow peak values in the 95PPU band are much lower than the observation data, except for M_{CHIRPS}, which indicates that the prediction uncertainty near streamflow peaks in this basin is significant, which may be caused by the uncertainties of precipitation inputs that propagate to the uncertainties of streamflow prediction (Neitsch *et al.* 2011).

CONCLUSIONS

Streamflow simulation of six sub-basins in the Shiyang River basin are investigated based on the SWAT model using the interpolation precipitation datasets of GSI, and the satellite and reanalysis precipitation datasets of TRMM, CMDF, CFSR, CHIRPS and PGF. The model performance, parameter sensitivity and uncertainty, and prediction uncertainty of streamflow simulation using the downscaled precipitation datasets, are discussed in detail. It is found that the model performance of streamflow simulation can be significantly improved by using the downscaled satellite or reanalysis precipitation datasets. For parameter optimization, the sensitivity and uncertainty of each parameter varies with precipitation datasets and sub-basins, and the parameter uncertainty with respect to different precipitation inputs can reflect the variation of simulation performance under multisource precipitation datasets. Among the model parameters, CN2 (the initial SCS runoff curve number for moisture condition II) and SMTMP (the base temperature of snow melt) are found to be of the highest relative sensitivities for most of the sub-basins, which suggests that the surface runoff and snowmelt are of significant importance for the streamflow production in Shiyang River basin. Moreover, M_{CHIRPS} and M_{PGF} are able to achieve acceptable uncertainties of streamflow predictions after parameter optimization, but the prediction uncertainty at streamflow peaks are not found to be negligible.

ACKNOWLEDGEMENTS

Financial support from the National Natural Science Foundation of China (No. 51279166 and No. 91425302) is acknowledged.

REFERENCES

Abbaspour, K. 2011 *SWAT-CUP4: SWAT Calibration and Uncertainty Programs – A User Manual*. Swiss Federal Institute of Aquatic Science and Technology, Eawag, Dübendorf, Switzerland.

Arnold, J. G., Moriasi, D. N., Gassman, P. W., Abbaspour, K. C., White, M. J., Srinivasan, R., Santhi, C., Harmel, R. D., Griensven, A. V., Liew, M. W. V., Kannan, N. & Jha, M. K. 2012 SWAT: model use, calibration, and validation. *Trans. ASABE* **55**, 1491–1508.

Beck, M. B. 1987 Water quality modeling: a review of the analysis of uncertainty. *Water Resour. Res.* **23** (8), 1393–1442.

Beven, K. 1993 Prophecy, reality and uncertainty in distributed hydrological modelling. *Adv. Water Resour.* **16** (1), 41–51.

Beven, K. J. & Binley, A. M. 1992 The future of distributed models: model calibration and uncertainty prediction. *Hydrol. Process.* **6** (3), 279–298.

Cecinati, F., Wani, O. & Rico-Ramirez, M. A. 2017 Comparing approaches to deal with non-gaussianity of rainfall data in kriging-based radar-gauge rainfall merging. *Water Resour. Res.* **53**, 1–20.

Daly, C., Neilson, P. & Phillips, D. 1994 A statistical-topographic model for mapping climatological precipitation over mountainous terrain. *J. Appl. Meteorol.* **33** (33), 140–158.

Dile, Y. T., Daggupati, P., George, C., Srinivasan, R. & Arnold, J. 2016 Introducing a new open source GIS user interface for the SWAT model. *Environ. Model. Softw.* **85**, 129–138.

Duan, Q., Sorooshian, S. & Gupta, V. 1992 Effective and efficient global optimization for conceptual rainfall–runoff models. *Water Resour. Res.* **28** (4), 1015–1031.

Duan, Z., Liu, J., Tuo, Y., Chiogna, G. & Disse, M. 2016 Evaluation of eight high spatial resolution gridded precipitation products in Adige Basin (Italy) at multiple temporal and spatial scales. *Sci. Total Environ.* **573**, 1536–1553.

Funk, C., Peterson, P., Landsfeld, M., Pedreros, D., Verdin, J., Shukla, S., Husak, G., Rowland, J., Harrison, L., Hoell, A. & Michaelsen, J. 2015 The climate hazards infrared precipitation with stations – a new environmental record for monitoring extremes. *Sci. Data* **2** (9), 150066.

He, M., Hogue, T. S., Franz, K. J., Margulis, S. A. & Vrugt, J. A. 2011 Characterizing parameter sensitivity and uncertainty for a snow model across hydroclimatic regimes. *Adv. Water Resour.* **34** (1), 114–127.

Hu, Q., Yang, D., Li, Z., Mishra, A. K., Wang, Y. & Yang, H. 2014 Multi-scale evaluation of six high-resolution satellite monthly rainfall estimates over a humid region in China with dense rain gauges. *Int. J. Remote Sens.* **35** (4), 1272–1294.

Huffman, G., Adler, R., Bolvin, D. T., Gu, G., Nelkin, E., Bowman, K., Hong, Y., Stocker, T. & Wolff, D. 2007 The TRMM multisatellite precipitation analysis (TMPA): quasi-global, multiyear, combined-sensor precipitation estimates at fine scales. *J. Hydrometeorol.* **8** (1), 38–55.

Jiang, S., Ren, L., Xu, C.-Y., Liu, S., Yuan, F. & Yang, X. 2018 Quantifying multi-source uncertainties in multi-model predictions using the Bayesian model averaging scheme. *Hydrol. Res.* **49** (3), 954–970.

Li, X. H., Zhang, Q. & Xu, C. Y. 2012 Suitability of the TRMM satellite rainfalls in driving a distributed hydrological model for water balance computations in Xinjiang catchment, Poyang lake basin. *J. Hydrol.* **426** (7), 28–38.

Liang, Z. M., Tang, T. T., Li, B. Q., Liu, T., Wang, J. & Hu, Y. M. 2018 Long-term streamflow forecasting using SWAT through the integration of the random forests precipitation generator: case study of Danjiangkou Reservoir. *Hydrol. Res.* **49** (5), 1513–1527.

Michaelides, S., Levizzani, V., Anagnostou, E., Bauer, P., Kasparis, T. & Lane, J. E. 2009 Precipitation: measurement, remote sensing, climatology and modeling. *Atmos. Res.* **94** (4), 512–533.

Misirli, F., Gupta, H. V., Sorooshian, S. & Thiemann, M. 2003 Bayesian recursive estimation of parameter and output uncertainty for watershed models. In: *Water Science and Application*, Vol. 6. (Q. Y. Duan, H. V. Gupta, S. Sorooshian, A. N. Rousseau & R. Turcotte, eds). American Geophysical Union, Washington DC, USA, pp. 113–124.

Moine, N. L., Hendrickx, F., Gailhard, J., Garçon, R. & Gottardi, F. 2015 Hydrologically aided interpolation of daily precipitation and temperature fields in a mesoscale alpine catchment. *J. Hydrometeorol.* **16** (6), 2595–2618.

Moriasi, D. N., Arnold, J. G., Liew, M. W. V., Bingner, R. L., Harmel, R. D. & Veith, T. L. 2007 Model evaluation guidelines for systematic quantification of accuracy in watershed simulations. *Trans. ASABE* **50** (3), 885–900.

Neitsch, S. L., Arnold, J. G., Kiniry, J. R. & Williams, J. R. 2011 *Soil and Water Assessment Tool – Theoretical Documentation Version 2009*. Technical Report No. 406. Agricultural Experiment Station, Temple, Texas.

Price, K., Purucker, S. T., Kraemer, S. R., Babendreier, J. E. & Knightes, C. D. 2014 Comparison of radar and gauge precipitation data in watershed models across varying spatial and temporal scales. *Hydrol. Process.* **28** (9), 3505–3520.

Saha, S., Moorthi, S., Pan, H. L., Wu, X., Wang, J., Nadiga, S., Tripp, P., Kistler, R., Woollen, J., Behringer, D., Liu, H., Stokes, D., Grumbine, R., Gayno, G., Wang, J., Hou, Y. T., Chuang, H. Y., Juang, H. M. H., Sela, J., Iredell, M., Treadon, R., Kleist, D., van Delst, P., Keyser, D., Derber, J., Ek, M., Meng, J., Wei, H., Yang, R., Lord, S., van den Dool, H., Kumar, A., Wang, W., Long, C., Chelliah, M., Xue, Y., Huang, B., Schemm, J. K., Ebisuzaki, W., Lin, R., Xie, P., Chen, M., Zhou, S., Higgins, W., Zou, C. Z., Liu, Q., Chen, Y., Han, Y., Cucurull, L., Reynolds, R. W., Rutledge, G. & Goldberg, M. 2010 The NCEP climate forecast system reanalysis. *B. Am. Meteorol. Soc.* **91** (8), 1015–1057.

Sheffield, J., Goteti, G. & Wood, E. F. 2006 Development of a 50-year high-resolution global dataset of meteorological forcings for land surface modeling. *J. Climate* **19** (13), 3088–3111.

Silva, R. M. D., Dantas, J. C., Beltrao, J. D. A. & Santos, C. A. G. 2018 Hydrological simulation in a tropical humid basin in the Cerrado biome using the SWAT model. *Hydrol. Res.* **49** (3), 908–923.

Teegavarapu, R. S. V. & Chandramouli, V. 2005 Improved weighting methods, deterministic and stochastic data-driven models for estimation of missing precipitation records. *J. Hydrol.* **312** (1–4), 191–206.

Wang, L. P., Ochoarodríguez, S., Onof, C. & Willems, P. 2015 Singularity-sensitive gauge-based radar rainfall adjustment methods for urban hydrological applications. *Hydrol. Earth Syst. Sci.* **12** (2), 1855–1900.

Wang, J. L., Chen, H., Xu, C. Y., Zeng, Q., Wang, Q. J., Kim, J. S., Chen, J. & Guo, S. L. 2018 Tracking the error sources of spatiotemporal differences in TRMM accuracy using error decomposition method. *Hydrol. Res.* **49** (6), 1960–1976.

Wyss, J., Williams, E. R. & Bras, R. L. 1990 Hydrologic modeling of New England river basins using radar rainfall data. *J. Geophys. Res. Atmos.* **95** (D3), 2143–2152.

First received 13 June 2018; accepted in revised form 16 January 2019. Available online 15 March 2019